

# Seven Years of Structure Functions

Keith Griffioen  
College of William & Mary

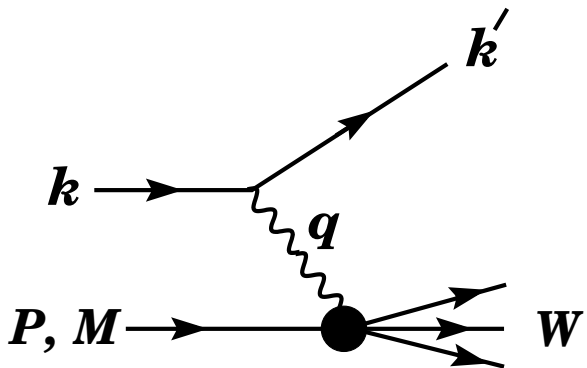
Highlights of the First Seven Years

Jefferson Lab Users Meeting

12 June 2003

- Introduction
- Unpolarized structure functions
- Tagged structure functions
- $g_1$ , asymmetries, and  $g_2$
- Moments
- Conclusions

## Kinematics



Lepton scattering is described by two variables  $\theta$  and  $E'$ , or Lorentz invariant combinations.

$k$  and  $k'$  are incident and final lepton 4-momenta.

$p$  is the initial nucleon 4-momentum.

$q$  is the 4-momentum of the transferred virtual photon.

$s_N$  and  $s_\ell$  are nucleon and lepton spin 4-vectors.

$M$  is the nucleon mass

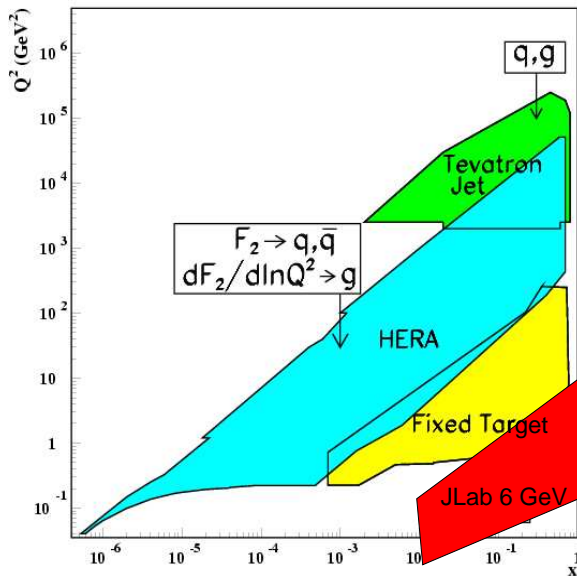
$$\frac{d^2\sigma}{dE'd\Omega} = \frac{e^4}{16\pi^2 Q^4} \left(\frac{E'}{E}\right) L^{\mu\nu} W_{\mu\nu}$$

$$L^{\mu\nu} = 2 [k'^\mu k^\nu + k'^\nu k^\mu - k \cdot k' g^{\mu\nu} - i\epsilon^{\mu\nu\rho\sigma} q_\rho s_{\ell\sigma}]$$

$$q^\mu W^{\mu\nu} = q^\nu W_{\mu\nu} = q_\mu L^{\mu\nu} = q_\nu L^{\mu\nu} = 0$$

$$\begin{aligned} W_{\mu\nu} = & -F_1 g_{\mu\nu} + \frac{F_2}{p \cdot q} p_\mu p_\nu + \frac{i g_1}{p \cdot q} \epsilon_{\mu\nu\rho\sigma} q^\rho s_N^\sigma + \\ & \frac{i g_2}{(p \cdot q)^2} \epsilon_{\mu\nu\rho\sigma} q^\rho (p \cdot q s_N^\sigma - s_N \cdot q p^\sigma) \end{aligned}$$

## Kinematics



Lorentz invariants:

$$\begin{aligned}\nu &= p \cdot q / M = (E - E')_{\text{lab}} \\ Q^2 &= -q \cdot q = (4EE' \sin^2 \frac{\theta}{2})_{\text{lab}} \\ x &= -q \cdot q / 2p \cdot q = (Q^2 / 2M\nu)_{\text{lab}} \\ y &= p \cdot q / p \cdot k = (\nu/E)_{\text{lab}} \\ W^2 &= (p + q)^2 = (M^2 + 2M\nu - Q^2)_{\text{lab}} \\ s &= (k + p)^2 = (2EM + M^2)_{\text{lab}}\end{aligned}$$

$$\frac{d^2\sigma}{dx dQ^2} = \frac{\pi\nu}{xE'E} \frac{d^2\sigma}{dE'd\Omega}$$

Variables of choice are  $(x, Q^2)$  for DIS and  $(W, Q^2)$  for resonance region.

## Structure Functions

Unpolarized Cross Section:

$$\frac{d^2\sigma}{dxdQ^2} = \frac{8\pi\alpha^2y}{Q^4} \left[ \frac{y}{2} F_1 + \frac{\xi}{2xy} F_2 \right]$$

Polarized Cross Section:

$$\begin{aligned} \frac{d^2\Delta\sigma}{dxdQ^2} = & \frac{8\pi\alpha^2y}{Q^4} \left[ \cos\alpha \left\{ (\xi + \frac{y}{2}) g_1 - \frac{\gamma y}{2} g_2 \right\} - \right. \\ & \left. \sin\alpha \cos\phi \sqrt{\gamma\xi} \left\{ \frac{y}{2} g_1 + g_2 \right\} \right] \end{aligned}$$

$\alpha$  = polar angle of target spin wrt the beam axis

$\phi$  = azimuthal spin angle wrt the scattering plane

$\alpha = 0^\circ$  (longitudinal);  $\alpha = 90^\circ, \phi = 0^\circ$  (transverse).

$$\gamma^2 = 4M^2x^2/Q^2 = Q^2/\nu^2$$

$$\xi = 1 - y - \gamma y^2/4$$

Parton Model:

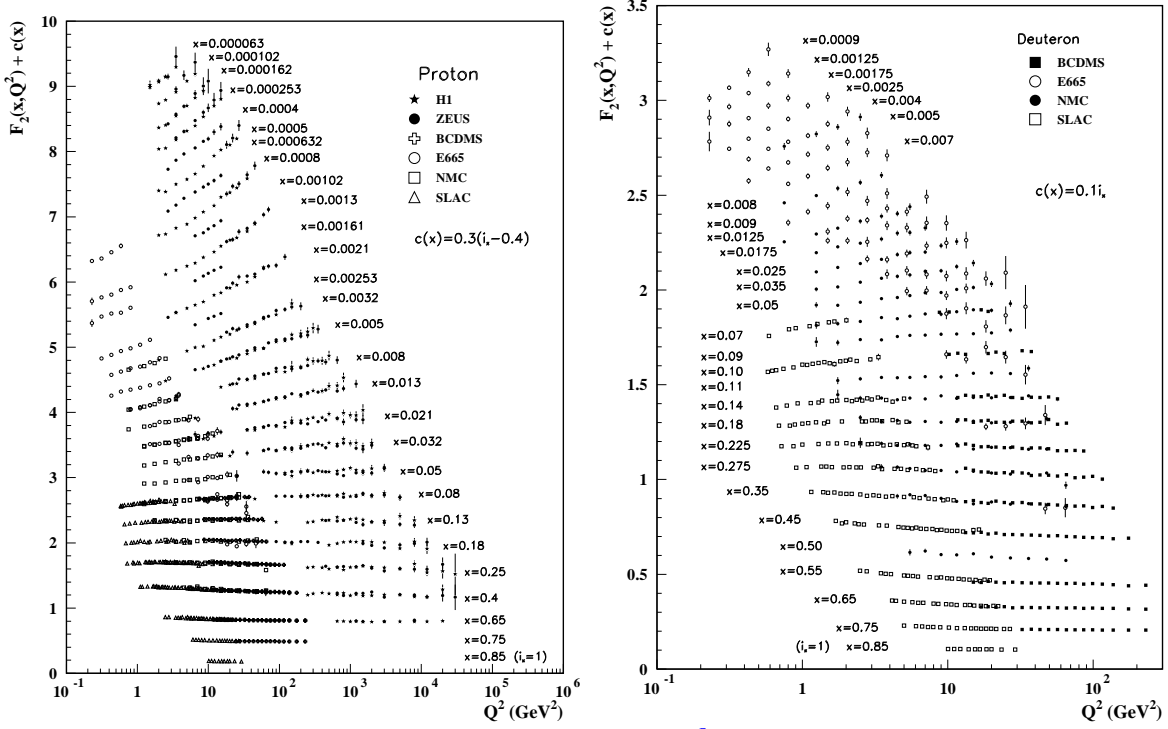
$$F_1(x, Q^2) = \frac{1}{2} \sum_i e_i^2 (q^\uparrow(x) + q^\downarrow(x) + \bar{q}^\uparrow(x) + \bar{q}^\downarrow(x))$$

$$F_2(x, Q^2) = 2x F_1(x, Q^2)$$

$$g_1(x, Q^2) = \frac{1}{2} \sum_i e_i^2 (q^\uparrow(x) - q^\downarrow(x) + \bar{q}^\uparrow(x) - \bar{q}^\downarrow(x))$$

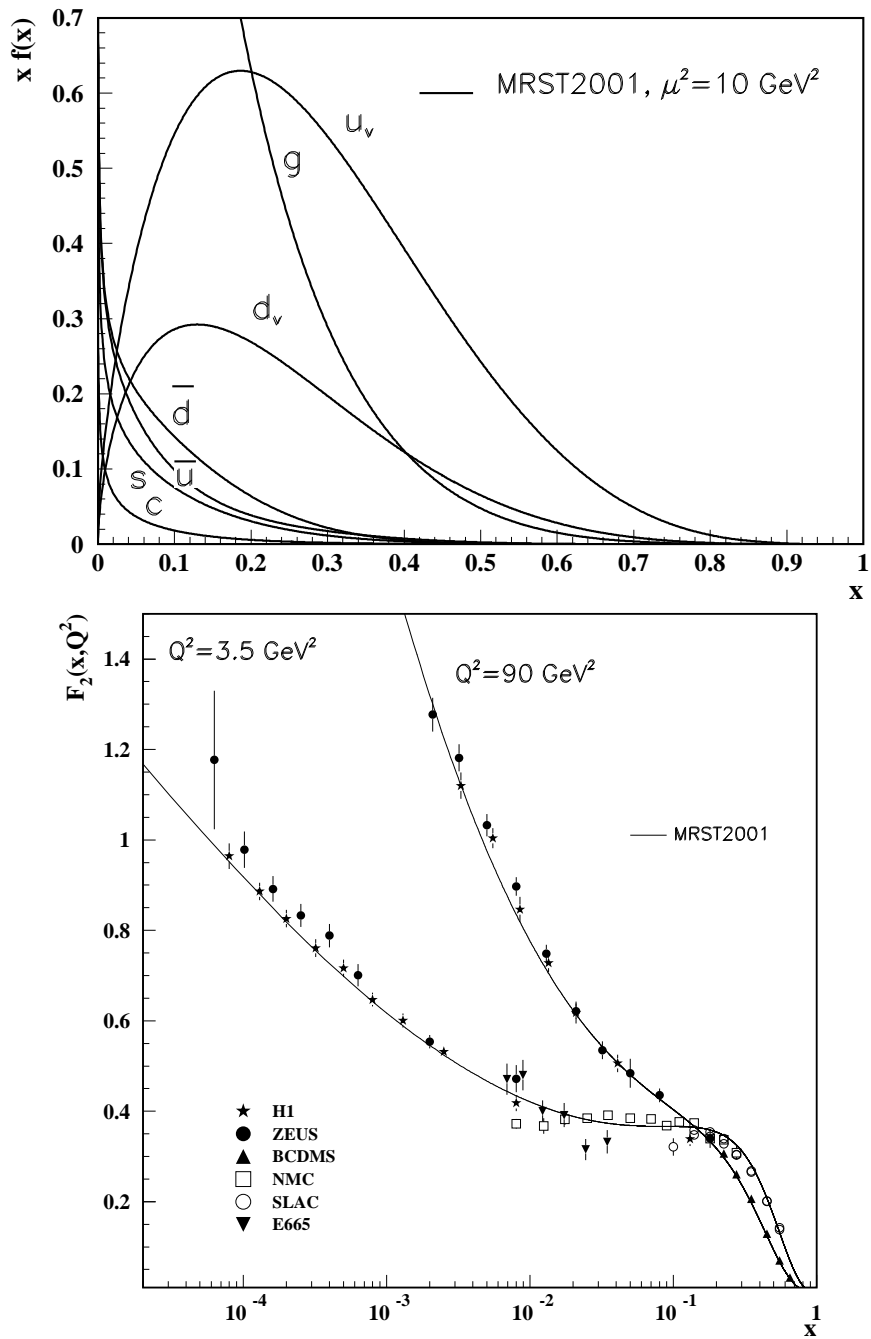
$$g_2(x, Q^2) = 0$$

## World Data on $F_2$

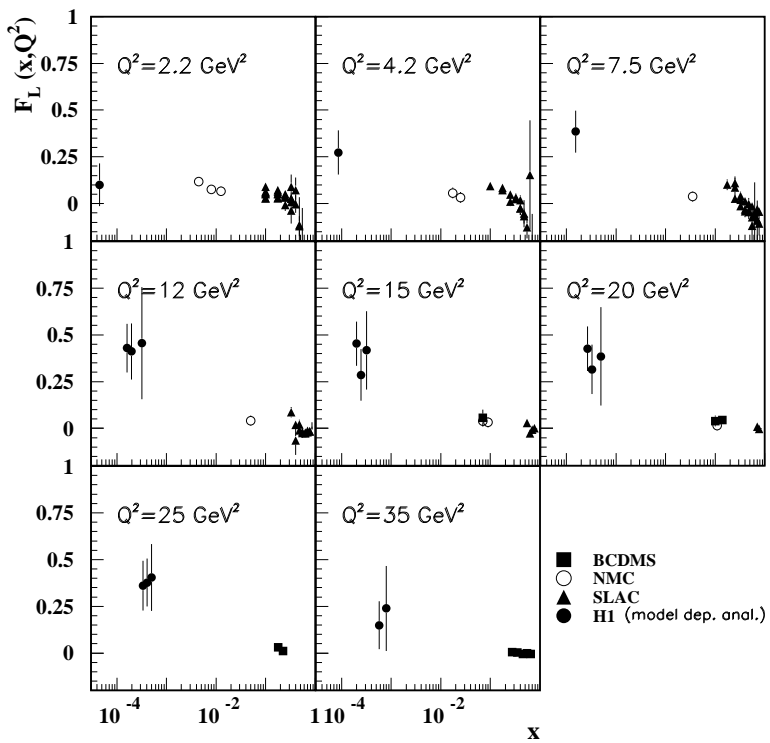


- $F_2(x)$  is not constant with  $Q^2$ , but exhibits scaling violations.
- Our microscope, with resolution  $1/Q$ , sees a bare quark clothed with the surrounding quarks and gluons.
- DGLAP equations describe QCD evolution of parton distributions:  $\partial q_i(x, Q^2)/\partial \ln Q^2 \sim \frac{\alpha_s(Q^2)}{2\pi} \int_x^1 \frac{dy}{y} P(y) \times q_i(\frac{x}{y}, Q^2)$  in which  $P(y)$  is the probability of a given parton splitting into two others.

# PDF

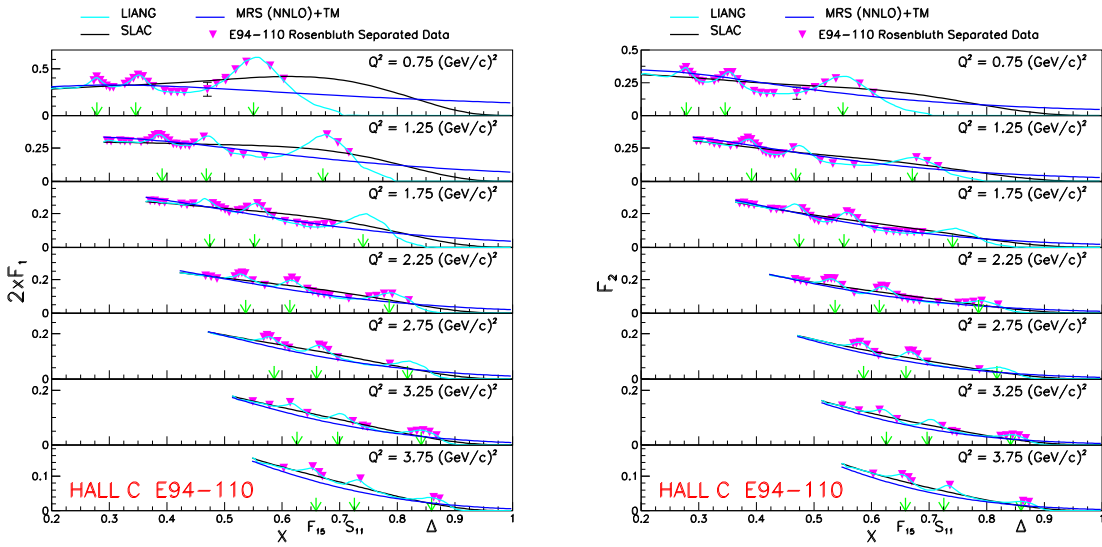


## $R$ and $F_L$



- $R(x, Q^2) = \sigma_L/\sigma_T = (1 + \gamma^2)F_2/2xF_1 - 1$
- $F_L(x, Q^2) = (1 + \gamma^2)F_2 - 2xF_1$
- Virtual photon polarization vectors for  $q_\mu = (q_0, 0, 0, q_3)$  are  $\epsilon_\pm^\mu = \frac{1}{\sqrt{2}}(0, \mp 1, -i, 0)$  for  $\pm$  helicity (transverse), and  $\epsilon_0^\mu = \frac{1}{Q}(q^3, 0, 0, q^0)$  (longitudinal).
- Both  $F_L$  and  $R$  vanish in the parton model.

## Hall C: E94-110



$$\frac{d^2\sigma}{dE'd\Omega} = \Gamma_V(\sigma_T + \epsilon\sigma_L)$$

$$1/\epsilon = 1 + 2(1 + 1/\gamma^2) \tan^2 \frac{\theta}{2}$$

$$\sigma_T = (\sigma_{1/2}^T + \sigma_{3/2}^T)/2 = N F_1$$

$$\sigma_{1/2}^T = N(F_1 + g_1 - \gamma^2 g_2) \propto |A_{1/2}|^2$$

$$\sigma_{3/2}^T = N(F_1 - g_1 + \gamma^2 g_2) \propto |A_{3/2}|^2$$

$$\sigma_{1/2}^L = \sigma_L = N F_L / 2x \propto |S_{1/2}|^2$$

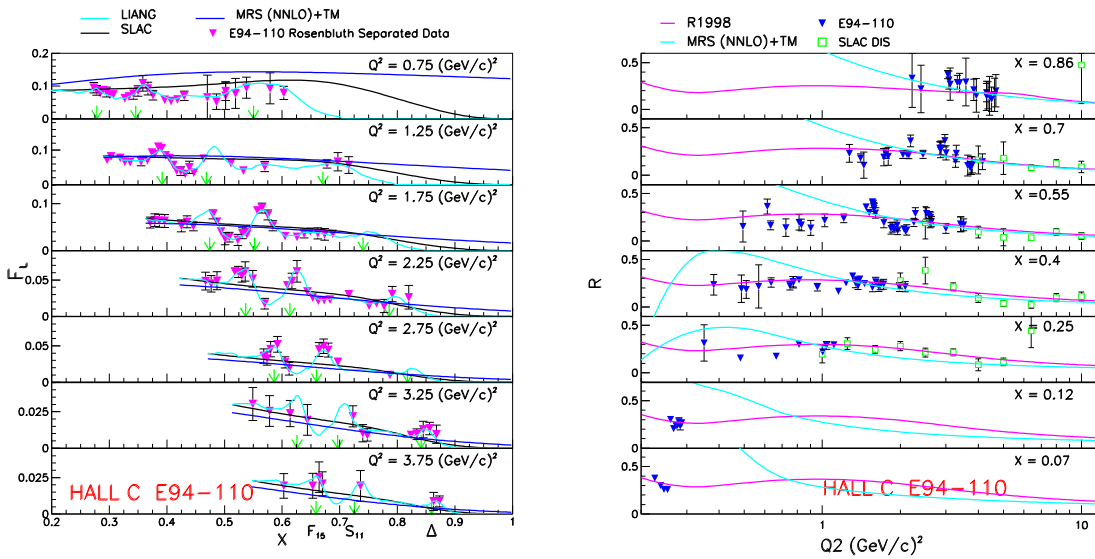
$$\sigma_{1/2}^{LT} = \sigma_{LT} = N \frac{Q}{M\nu} (g_1 + g_2) \propto S_{1/2}^* A_{1/2}$$

$$N = \frac{4\pi^2 \alpha}{KM}$$

$$\Gamma_V = \frac{\alpha K E'}{2\pi^2 Q^2 E(1-\epsilon)}$$

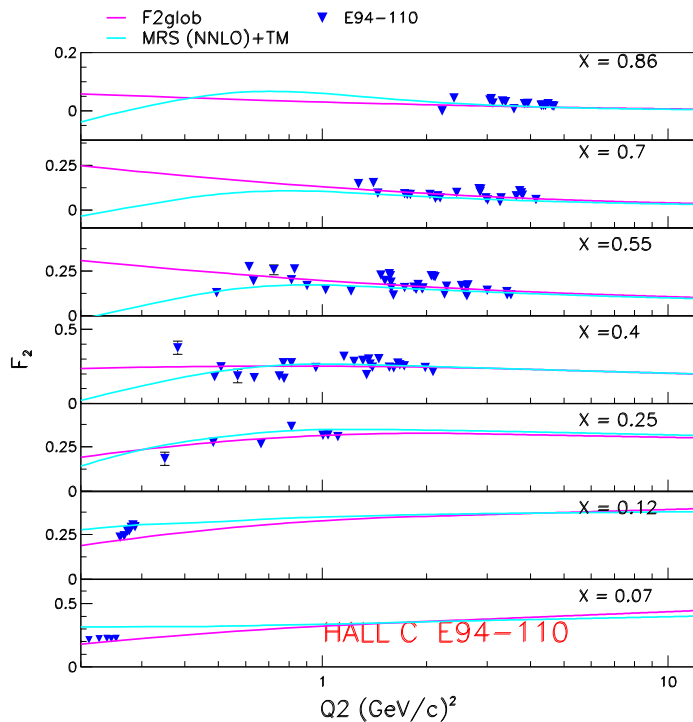
Rosenbluth separation gives  $\sigma_T$  and  $\sigma_L$ .

## Hall C: E94-110



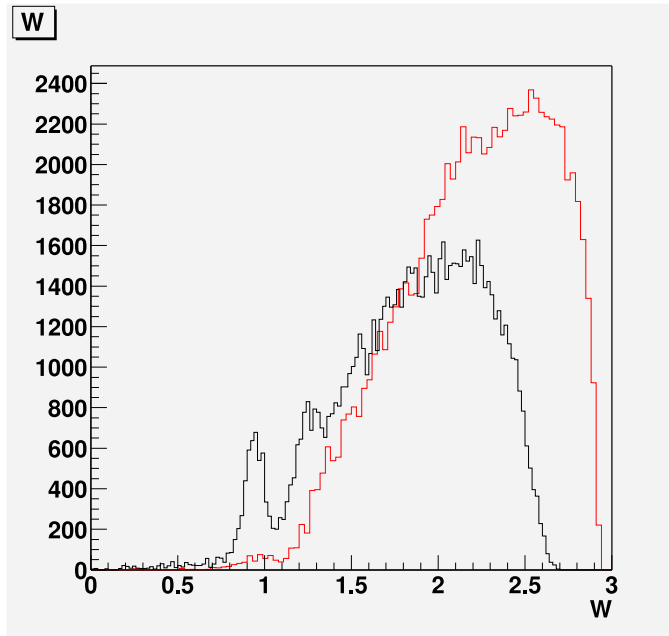
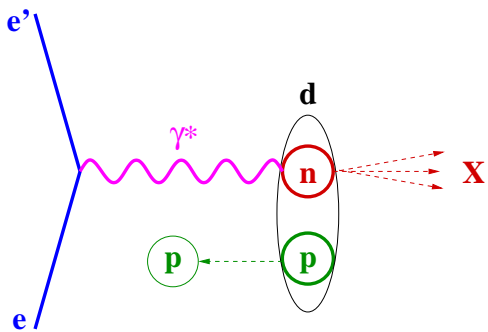
- Both  $F_L$  and  $R$  are positive and get smaller slowly with  $Q^2$ .
- Resonances show up as bumps that move with  $x$  as  $Q^2$  increases.
- New global parametrization fits the  $Q^2$  dependence for each bin in  $W$ .
- DIS extrapolations do well on average in the resonance region (duality).
- The DIS R1998 fit to  $R$  does extremely well with the new data, whereas NNLO extrapolations fail.

## Hall C: E94-110



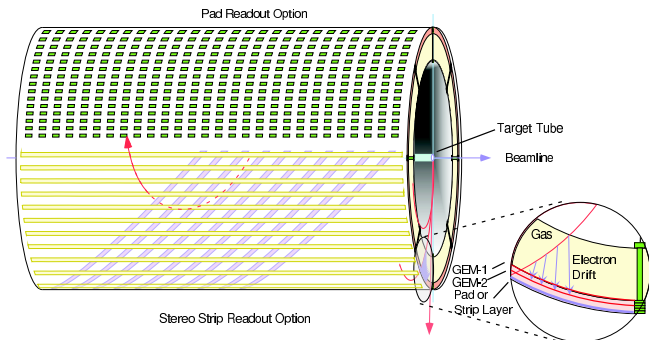
- Old SLAC parametrization does well.
- NNLO QCD fit also generally agrees with the  $Q^2$  dependence when corrected for target-mass effects.
- Data at low  $Q^2$  are often plotted versus Nachtmann  $\xi = 2x/(1 + \sqrt{1 + 4M^2x^2/Q^2})$  to correct for target-mass. Because there are scaling violations at all  $Q^2$ , one might prefer to use  $(x, Q^2)$  consistently.

## CLAS E94-102: $d(e, e' p_s)$



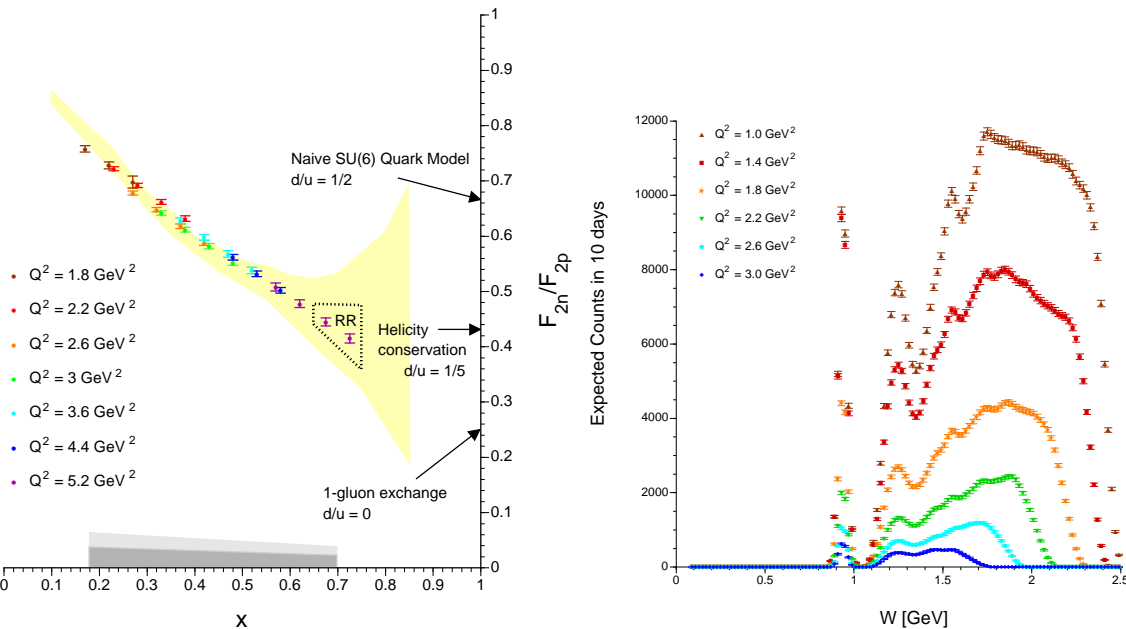
- At 6 GeV, CLAS can measure into the deep-inelastic region.
- Measures the neutron structure function for high ( $> 250$  MeV/c) momentum spectators; study off-shell effects and modifications to the structure functions when two nucleons are close
- Red curve: inclusive data from the deuteron target with elastic and resonances smeared out.
- Black curve:  $(e, e' p_s)$  data corrected for the neutron momentum before scattering. Peaks appear!

## CLAS E03-012: BONUS



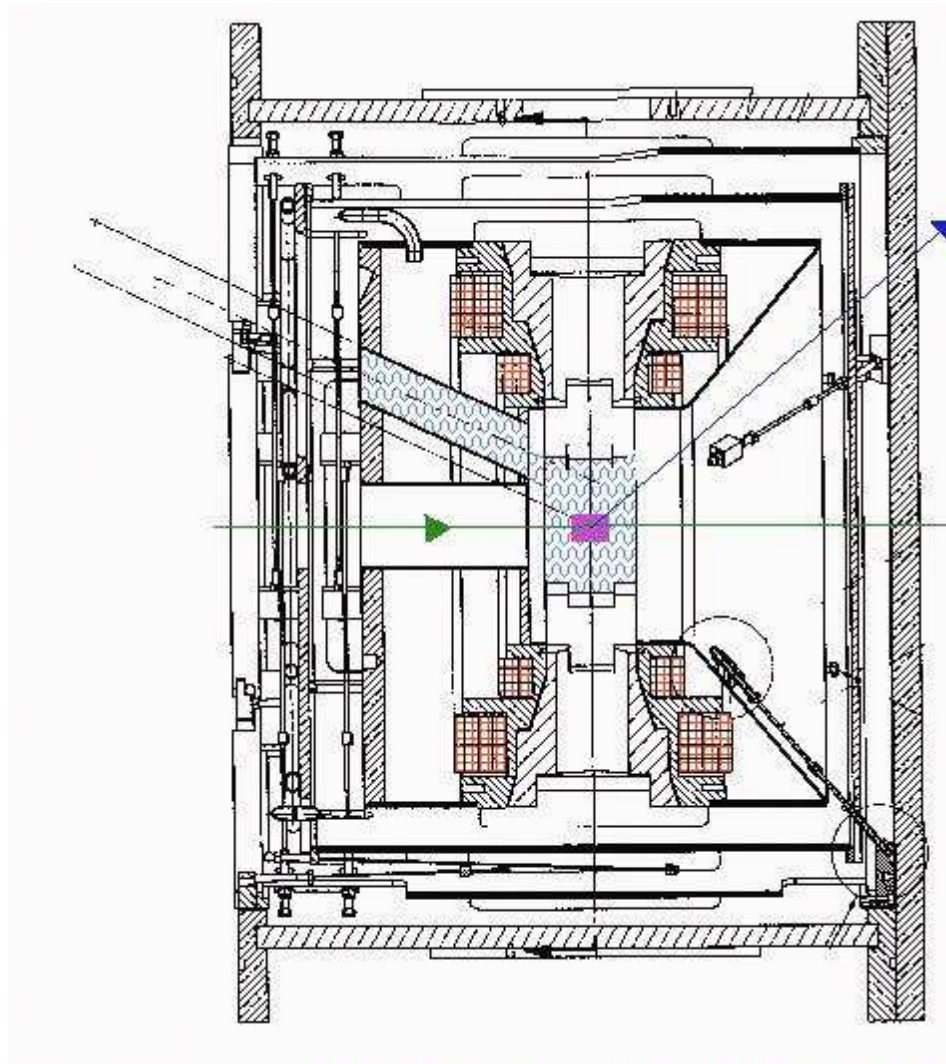
- Low-energy proton spectators from deuterium are hard to detect because of energy loss in the target.
- Slow spectators imply the neutron and proton are on average far apart (barely bound).
- Tagging slow protons from deuterium allows one to create a nearly free neutron target.
- Gaseous deuterium target; radial time projection chamber; gas electron multiplier (GEM) readout.

# CLAS BONUS



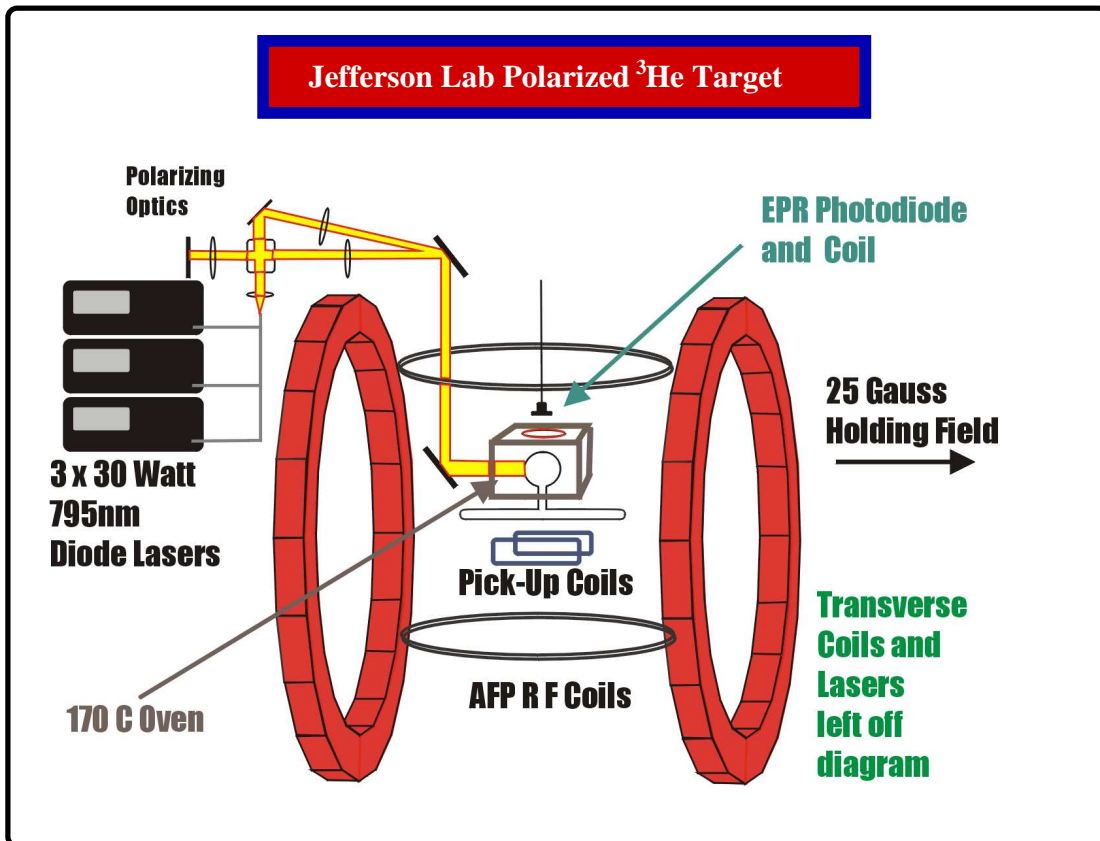
- Tagged structure functions corrected for nucleon motion show sharp peaks for elastic and resonances (right curve, expected results).
- Barely Offshell NUcleon Structure (BONUS) experiment will measure neutron structure functions without the usual proton contamination and smearing from deuterium.
- This method is especially useful at high  $x$  where model uncertainties dominate the extraction of  $F_2^n$ .
- This technique is easily extended to 12 GeV beams.

## CLAS Polarized Target

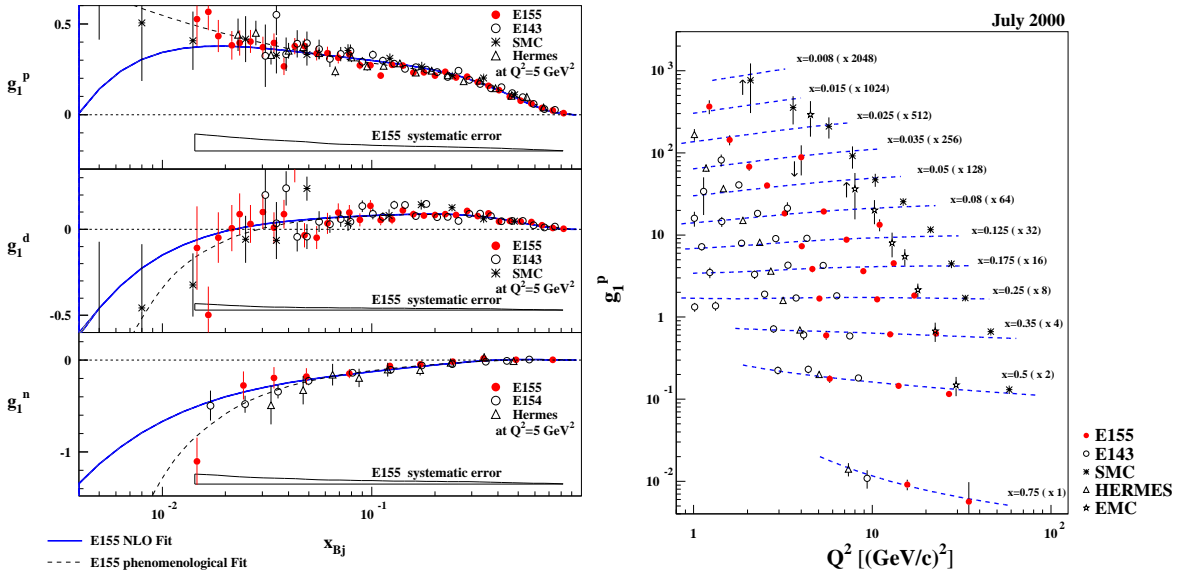


- Targets of  $^{15}\text{NH}_3$  and  $^{15}\text{ND}_3$ , 1 cm long, 1.5 cm diameter; 1 K, 5 T field, dynamic nuclear polarization.
- $P_t \approx 50\text{--}80\%$  for proton;  $P_t \approx 10\text{--}35\%$  for deuteron.

# Hall A Polarized Target



$$g_1(x, Q^2)$$



$$\left( \frac{d^2 \Delta \sigma}{dE' d\Omega} \right)_{\parallel} = 2\Gamma_V D (1 + \epsilon R) [\sigma_{TT} + \eta \sigma_{LT}]$$

$$\left( \frac{d^2 \Delta \sigma}{dE' d\Omega} \right)_{\perp} = 2\Gamma_V d (1 + \epsilon R) [\sigma_{LT} - \zeta \sigma_{TT}]$$

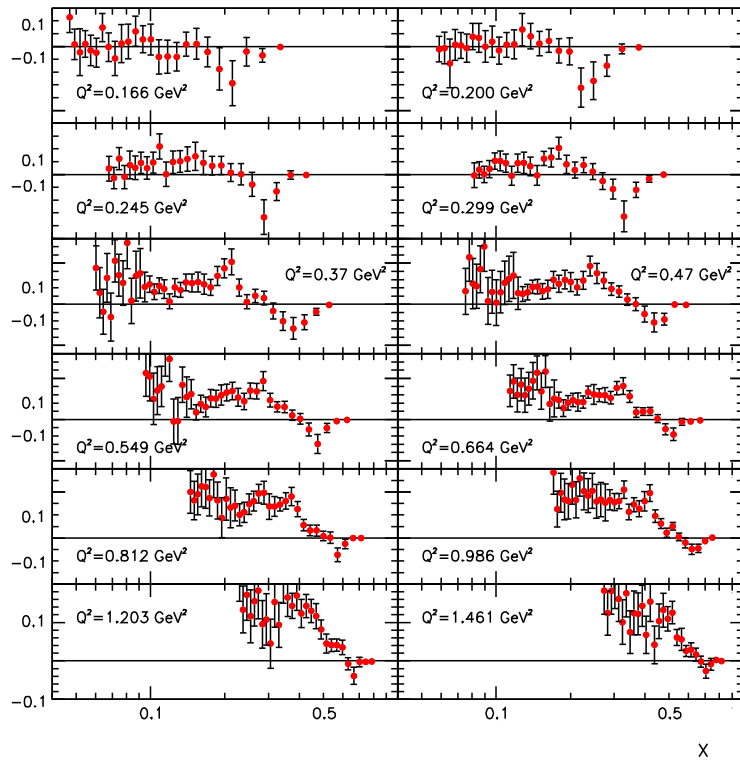
$D$  and  $d$  are depolarization factors.

$\eta$  and  $\zeta$  are kinematic factors (small).

$$\sigma_{TT} = (\sigma_{1/2}^T - \sigma_{3/2}^T)/2 = N(g_1 - \gamma^2 g_2).$$

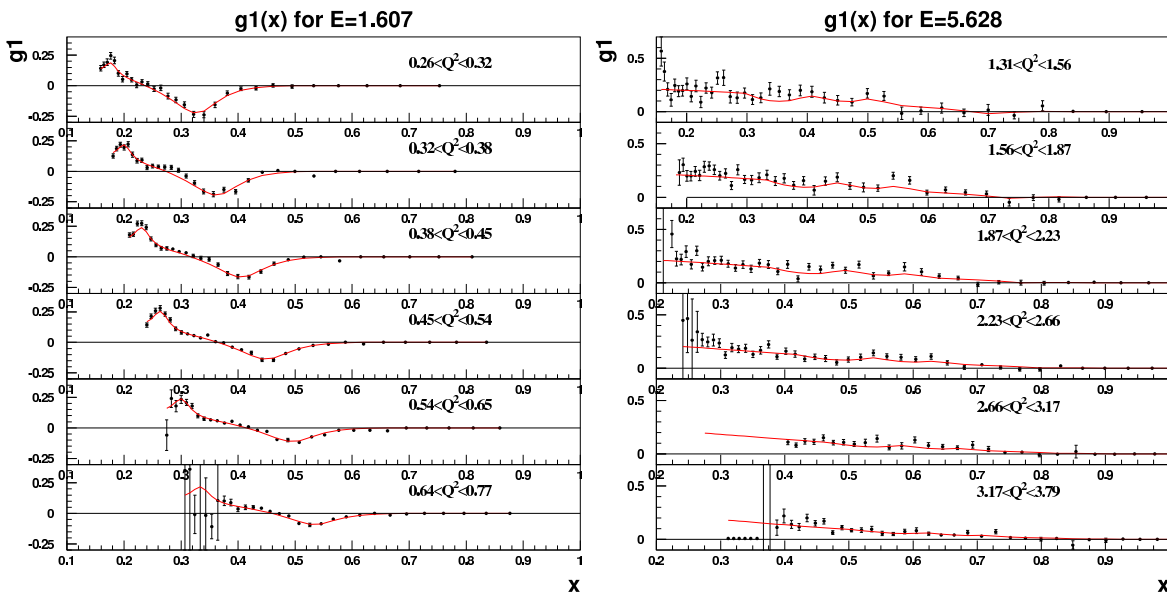
- Both  $\parallel$  and  $\perp$  data are necessary to extract  $g_1$
- $Q^2$  evolution similar to the unpolarized case.
- Consistent NLO analysis of world's data:  $\Delta\Sigma = 0.23 \pm 0.07$  and  $\Delta G = 1.6 \pm 0.8 \pm 1.1$

## CLAS (eg1a) $g_1^p$ vs. $x$



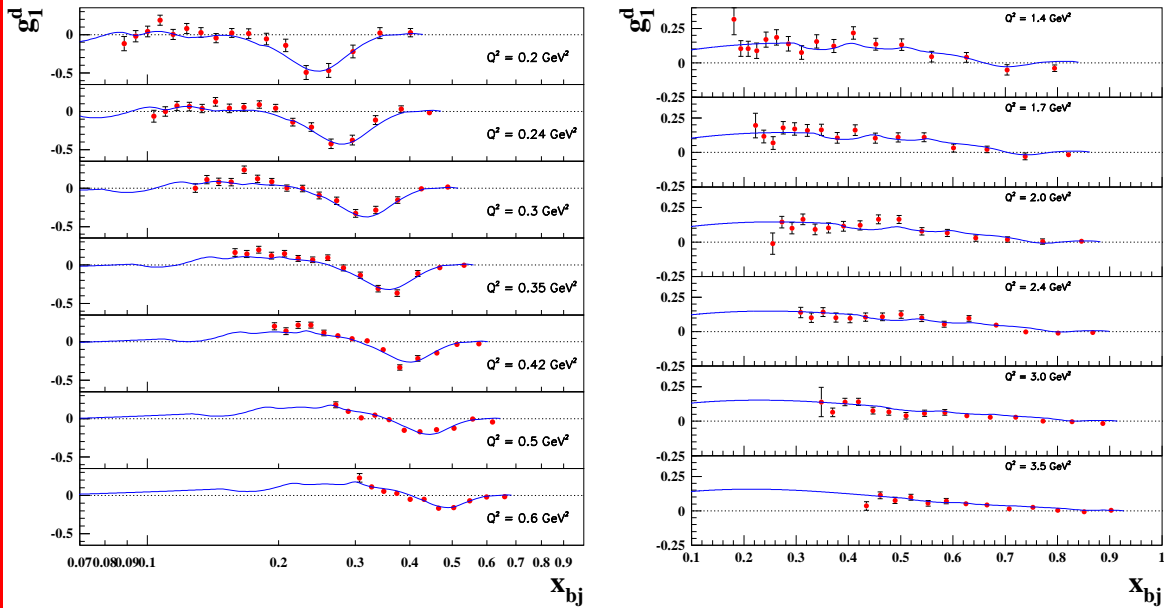
- CLAS has extended the measurements of  $g_1$  into the resonance region.
- The  $\Delta$  resonance, which moves upward in  $x$  with increasing  $Q^2$ , drives  $g_1$  negative.
- By comparison,  $g_1$  is always positive for DIS.

## CLAS (eg1b) $g_1^p$ vs. $x$

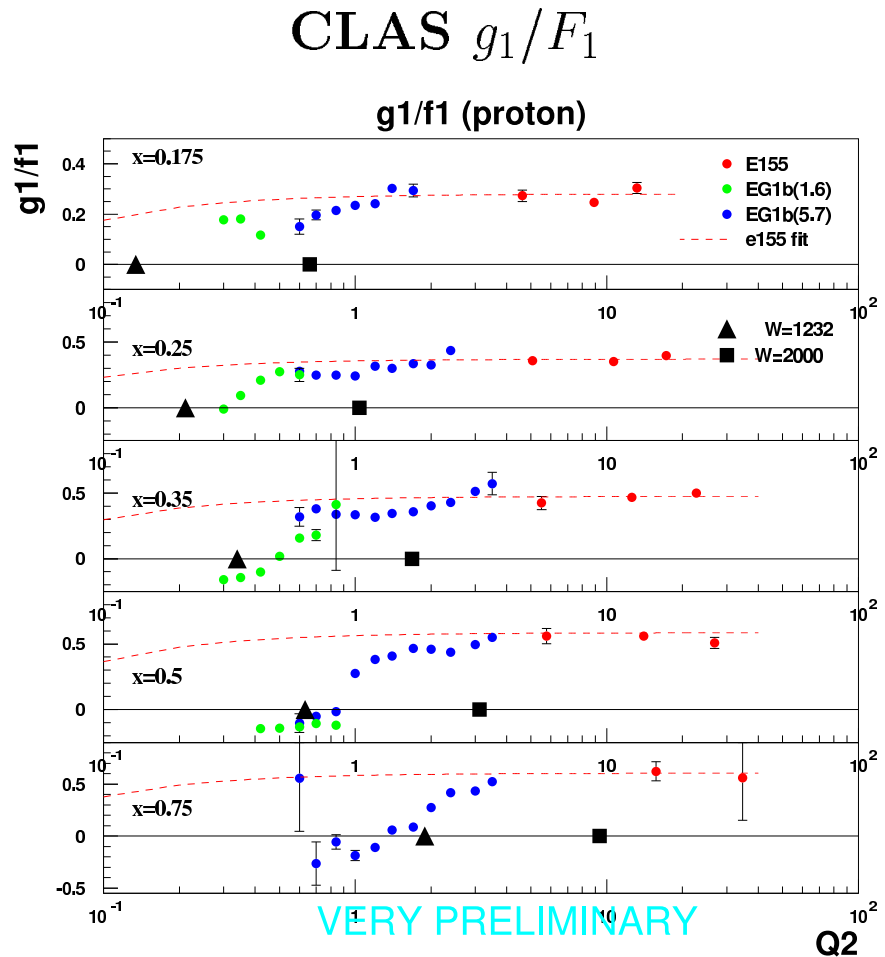


- Additional CLAS data have been taken at lower and higher energies for more complete kinematic coverage.
- For the 5.6 GeV data,  $g_1$  is positive.
- The  $\Delta$  drives the 1.6 GeV data negative.
- The newer data generally extend to lower  $x$ , and require less extrapolation when calculating moments.

## CLAS (eg1b) $g_1^d$ vs. $x$

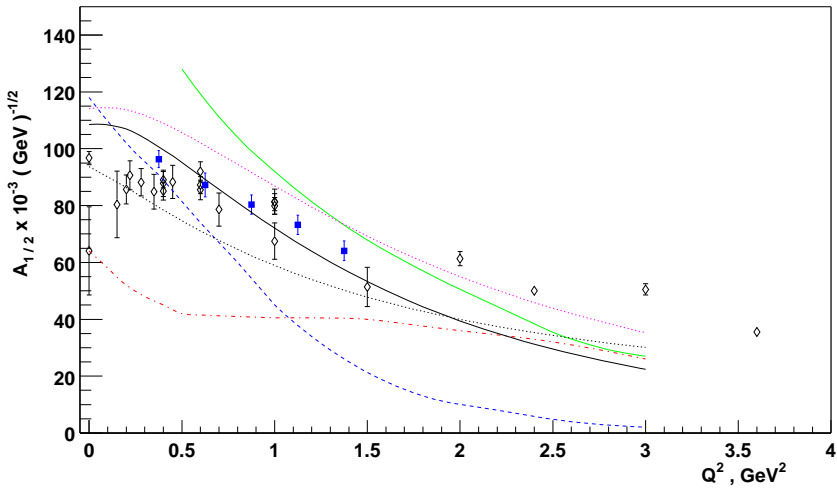


- CLAS took data with both  $\text{NH}_3$  and  $\text{ND}_3$  targets.
- The deuteron data show the same negative  $g_1$  for the  $\Delta$ , which disappears at higher  $Q^2$ .
- The model is a hybrid: DIS fits to data; resonance calculations using AO with helicity amplitudes modified to fit data; smooth interpolation between the two regions.

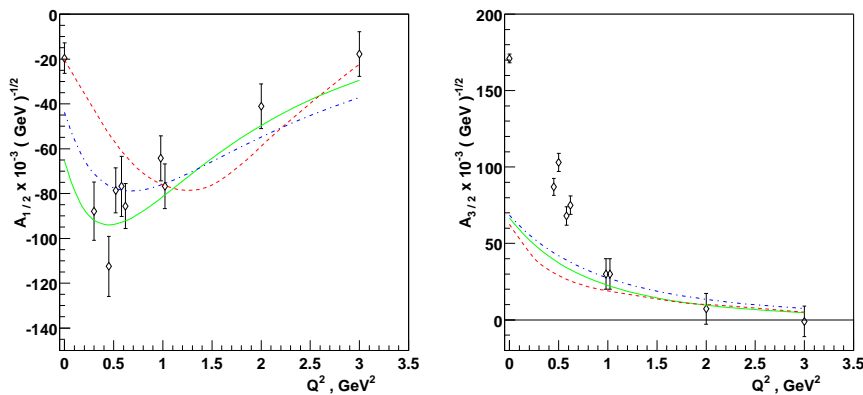


- For DIS,  $g_1$  scales almost like  $F_1$ , and  $g_1/F_1$  is nearly flat.
- The resonance structure causes  $g_1$  to evolve very differently from  $F_1$  at low  $Q^2$ .
- $g_1/F_1$  goes negative at the  $\Delta$  resonance.

## $S_{11}$ and $D_{13}$ Amplitudes



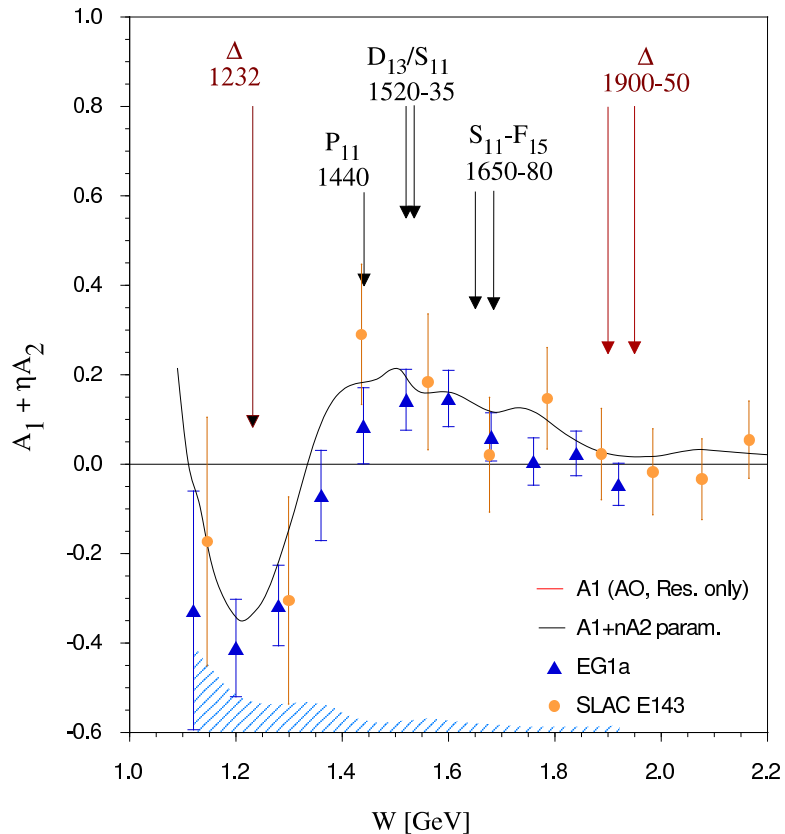
$A_{1/2}$  for the  $S_{11}(1535)$  Resonance



$A_{1/2}$  and  $A_{3/2}$  for the  $D_{13}(1520)$  Resonance

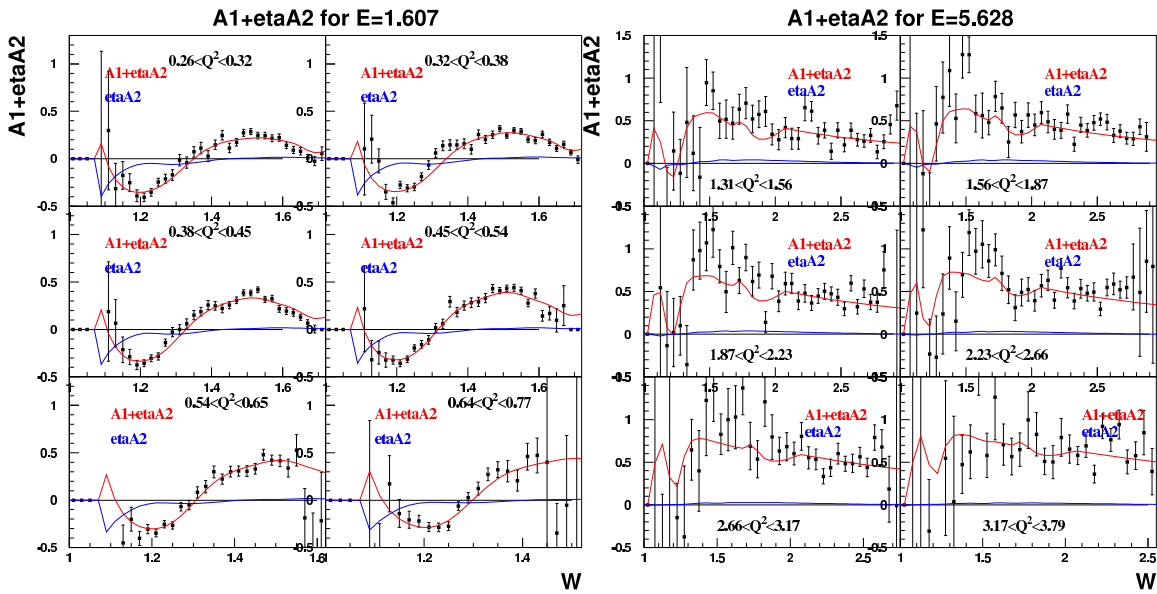
$$A_1 = \frac{|A_{1/2}|^2 - |A_{3/2}|^2}{|A_{1/2}|^2 + |A_{3/2}|^2}$$

## CLAS (eg1a) $A_1 + \eta A_2$ for p



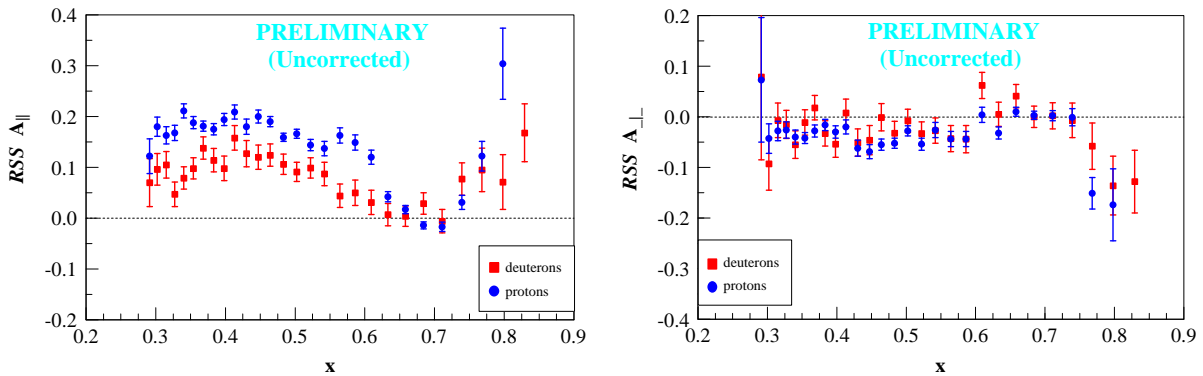
- CLAS can only measure  $\parallel$  spin configurations.
- Therefore,  $A_1 = \sigma_{TT}/\sigma_T$  cannot be separated from  $A_2 = \sigma_{LT}/\sigma_T$ .
- $\eta$  is generally small, so  $A_1$  dominates.

## CLAS (eg1b) $A_1 + \eta A_2$ vs. $x$ for p



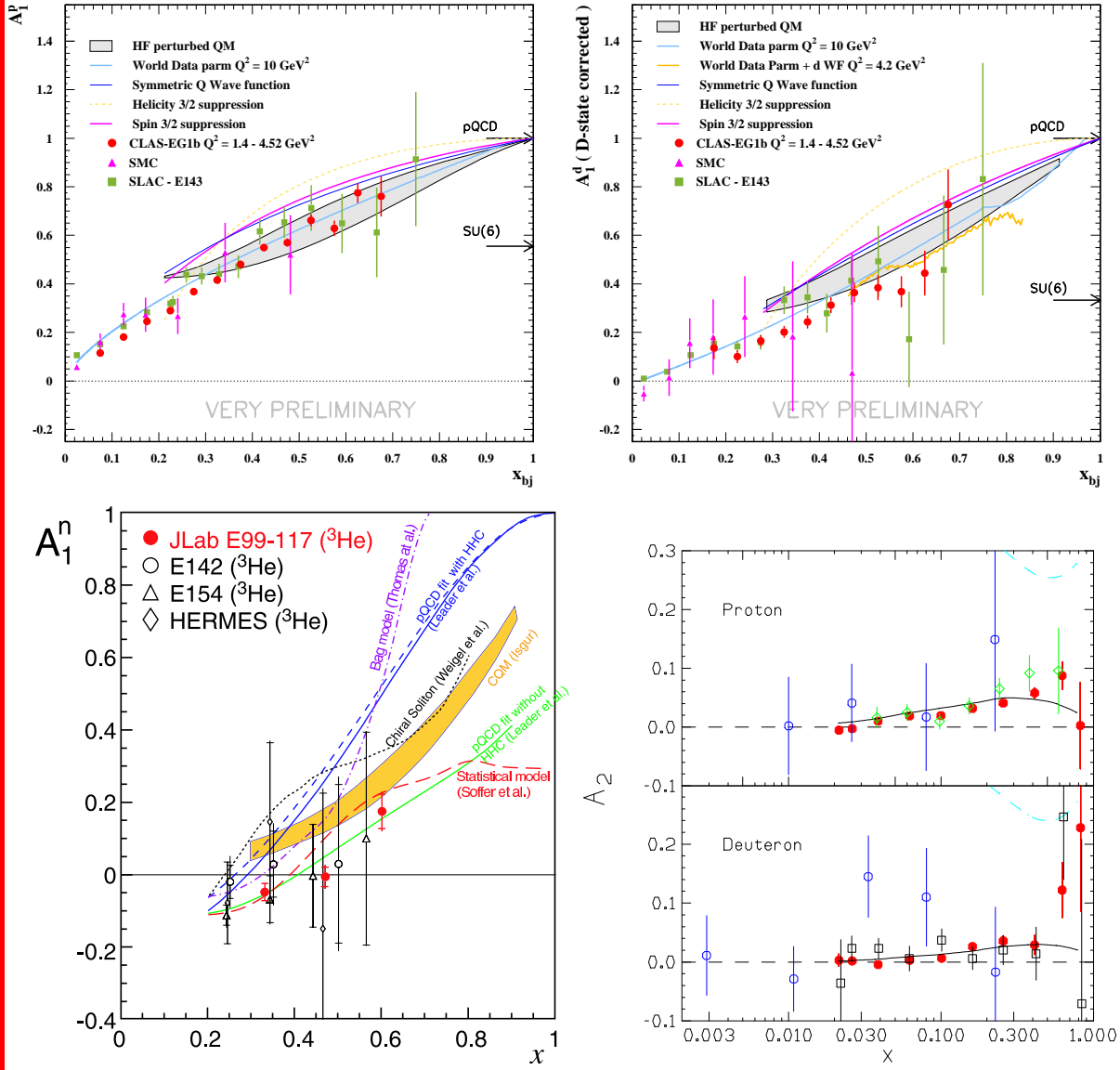
- Red curve: hybrid model
- Blue curve: estimate of  $\eta A_2$  from hybrid model.
- Plotted versus  $W$ , the data show resonance structure at fixed positions.

# Hall C E01-006 Resonance Spin Structure



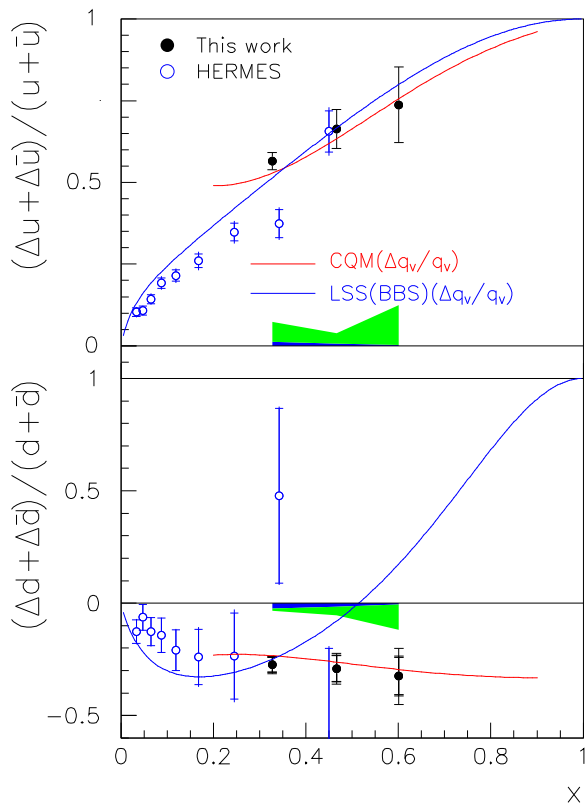
- Beam energy 5.755 GeV.
- HMS spectrometer at  $13.08^\circ$ .
- $\langle Q^2 \rangle = 1.3 \text{ GeV}^2$ .
- First JLab measurement using ammonia targets to measure  $\perp$  configuration.

## $A_1$ and $A_2$ vs. $x$



CLAS:  $p$  and  $d$ ; Hall A E99-117:  $n$ ; SLAC E155x:  $A_2$ .

## Hall A



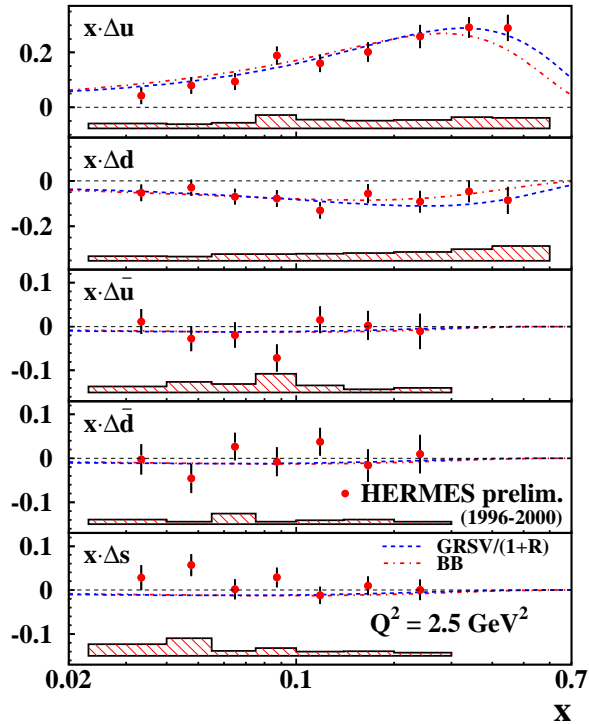
Assume no strange quarks for  $x > 0.3$  and no  $Q^2$ -dependence of  $A_1$

$$\frac{\Delta u}{u} = \frac{4}{15} \frac{g_1^p}{F_1^p} (4 + R) - \frac{1}{15} \frac{g_1^n}{F_1^n} (1 + 4R)$$

$$\frac{\Delta d}{d} = \frac{4}{15} \frac{g_1^n}{F_1^n} (4 + 1/R) - \frac{1}{15} \frac{g_1^p}{F_1^p} (1 + 4/R)$$

$$R \equiv d/u$$

## DIS Hadron Tagging



$$\sigma^h(x, Q^2, z) \propto \sum_i e_i^2 q_i(x, Q^2) D_i^h(z, Q^2)$$

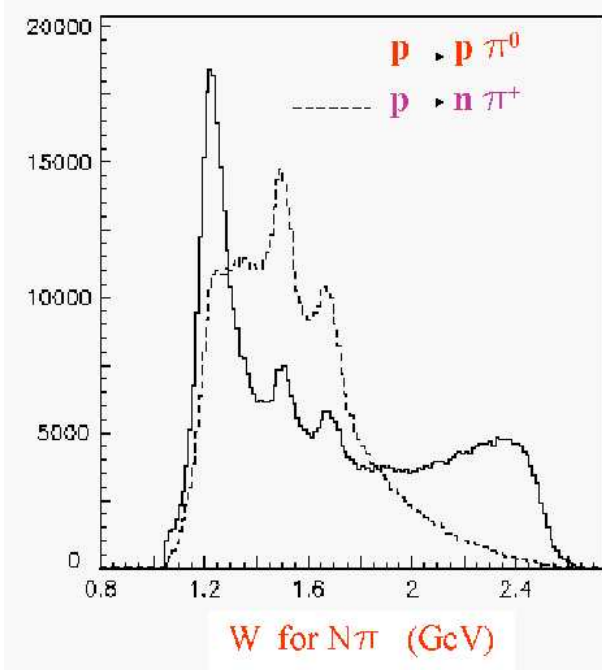
$$z = E_h/\nu$$

$$g_1/F_1 = \frac{\sum_i \Delta q_i(x, Q^2) \int_{z_{\min}}^{z_{\max}} dz D_i^h(z, Q^2)}{\sum_i q_i(x, Q^2) \int_{z_{\min}}^{z_{\max}} dz D_i^h(z, Q^2)}$$

$\Delta q/q$  extracted from semi-inclusive data, given knowledge of the fragmentation functions  $D_i^h$ .

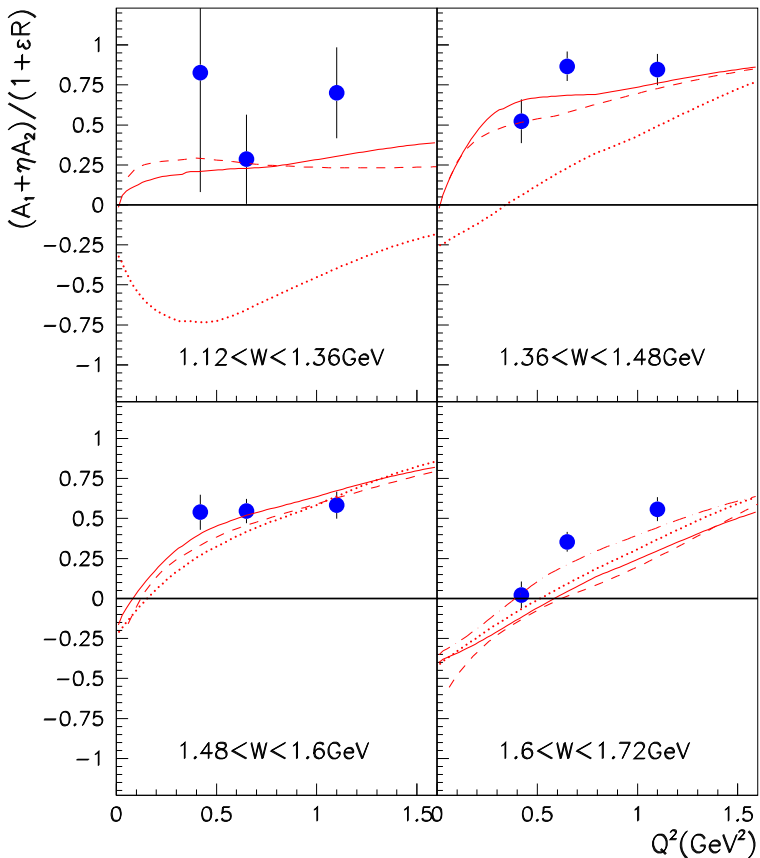
- Data from HERMES
- CLAS eg1 will also be able to do this analysis.

## Tagging with a $\pi$ : Isospin Differences



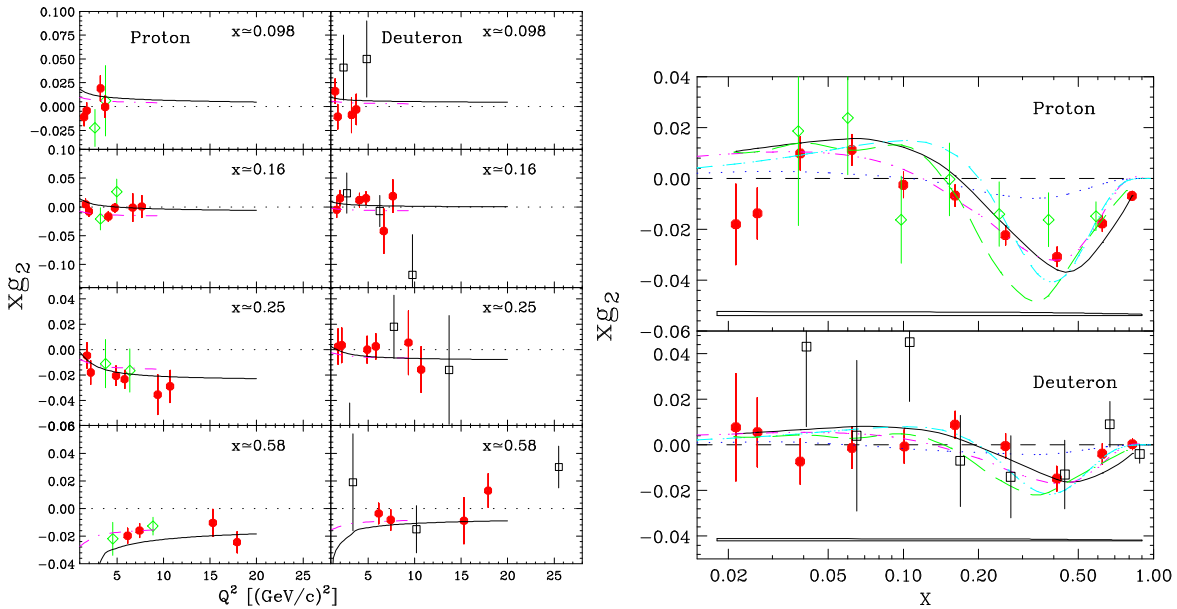
- Raw counts for  $ep \rightarrow ep\pi^0$  and  $ep \rightarrow en\pi^+$
- $$|\frac{3}{2}\frac{1}{2}\rangle = \sqrt{\frac{1}{3}}|n\pi^+\rangle + \sqrt{\frac{2}{3}}|p\pi^0\rangle$$
$$|\frac{1}{2}\frac{1}{2}\rangle = \sqrt{\frac{2}{3}}|n\pi^+\rangle - \sqrt{\frac{1}{3}}|p\pi^0\rangle$$
  - $p\pi^0$  emphasizes isospin  $T = \frac{3}{2}$  states
  - $n\pi^+$  emphasizes isospin  $T = \frac{1}{2}$  states

## CLAS $A_1 + \eta A_2$ versus $Q^2$ from $\pi^+n$



- Integrated over  $\cos \theta^*$
- AO resonance (dotted) [PRD47(93)46]
- AO full (solid)
- AO with  $A_1^{F15}$  increased by 0.4 (dot-dashed)
- MAID2000 [NPA645(99)145]

## SLAC E155x

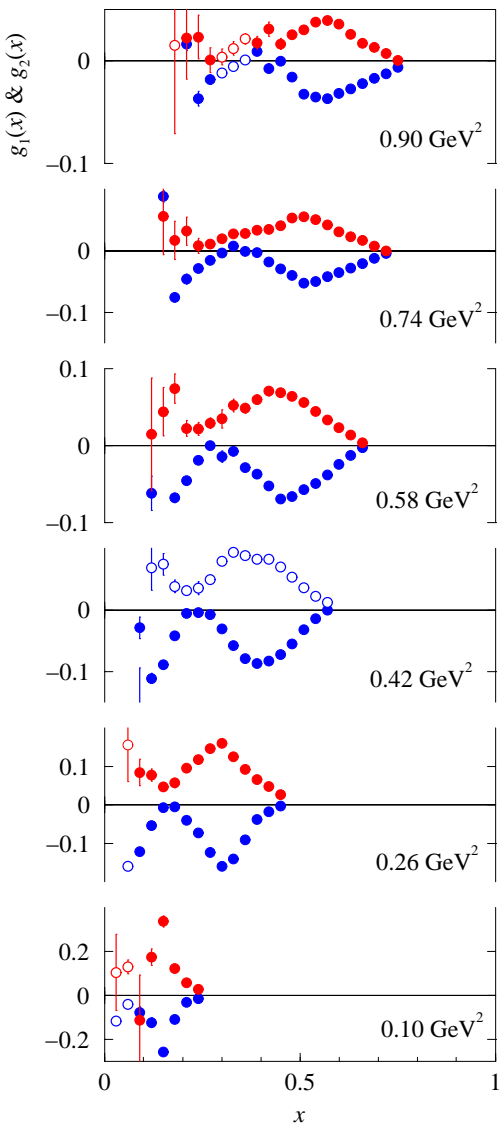


- Dedicated SLAC run to measure  $g_2$ .
- Improved on previous errors by over a factor of 3.
- $g_2^{WW} = -g_1(x, Q^2) + \int_x^1 \frac{g_1(y)}{y} dy$
- $\bar{g}_2 = g_2 - g_2^{WW}$  (higher twist component)
- Solid line shows  $g_2^{WW}$
- Enough data exist to get a rough idea of the  $Q^2$  evolution.

## Hall A E94-010: $g_1^{^3\text{He}}$ and $g_2^{^3\text{He}}$

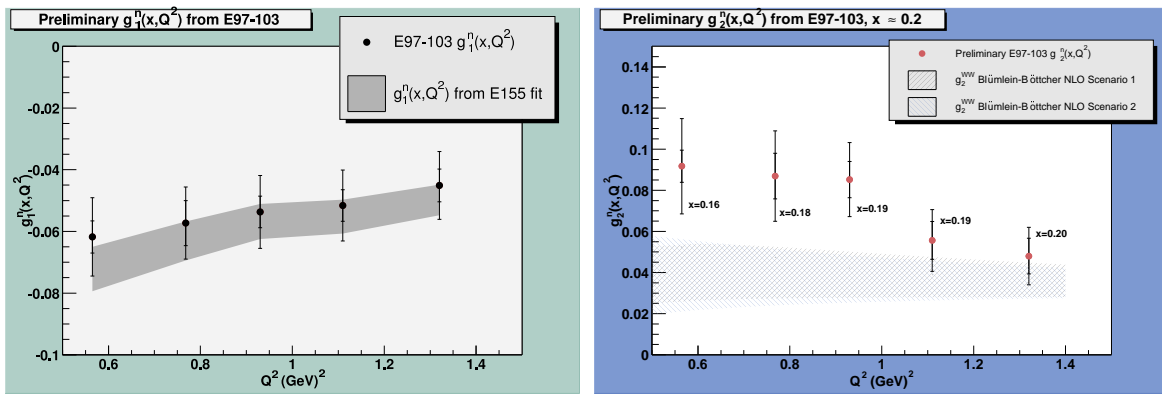
Polarized  ${}^3\text{He}$  target  
enables measurement of  
 $\parallel$  and  $\perp$  asymmetries  
in the same experiment.

$g_2 \approx -g_1$   
(i.e.  $\sigma_{LT} \approx 0$ )



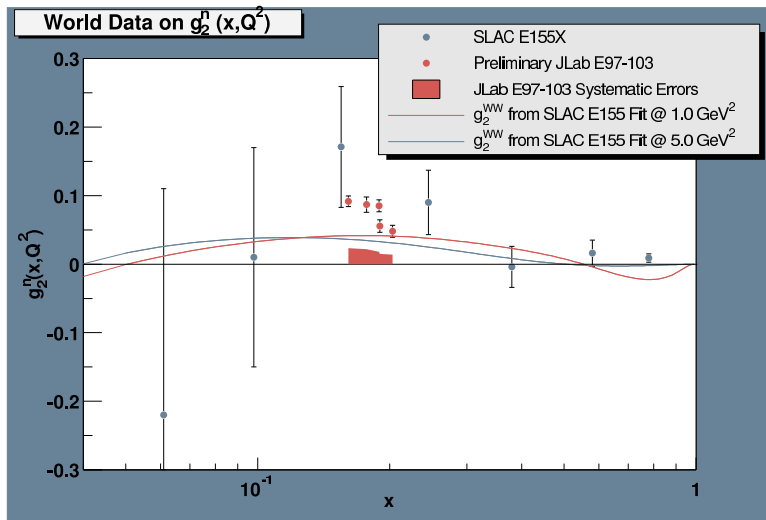
# Hall A: E97-103

## Search for Higher Twist Effects in the Neutron Structure Function $g_2^n(x, Q^2)$



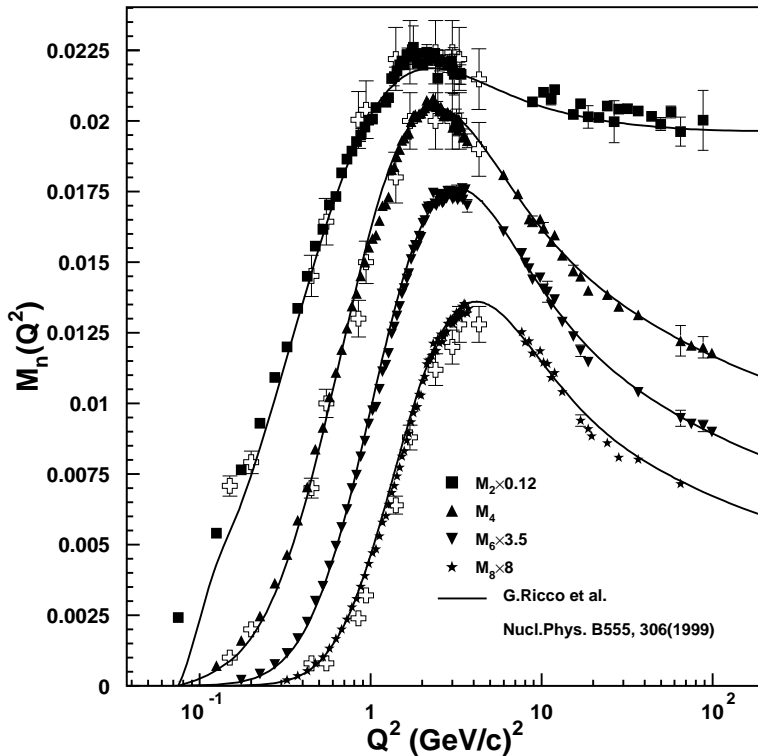
- Precision measurement of both  $g_1^n$  and  $g_2^n$  at  $x \approx 0.2$  using the polarized  ${}^3\text{He}$  target in Hall A.
- Systematics of  $g_1$  agree with the E155 fit.
- $g_2$  is generally above the  $g_2^{WW}$  estimates.

## Hall A E97-103



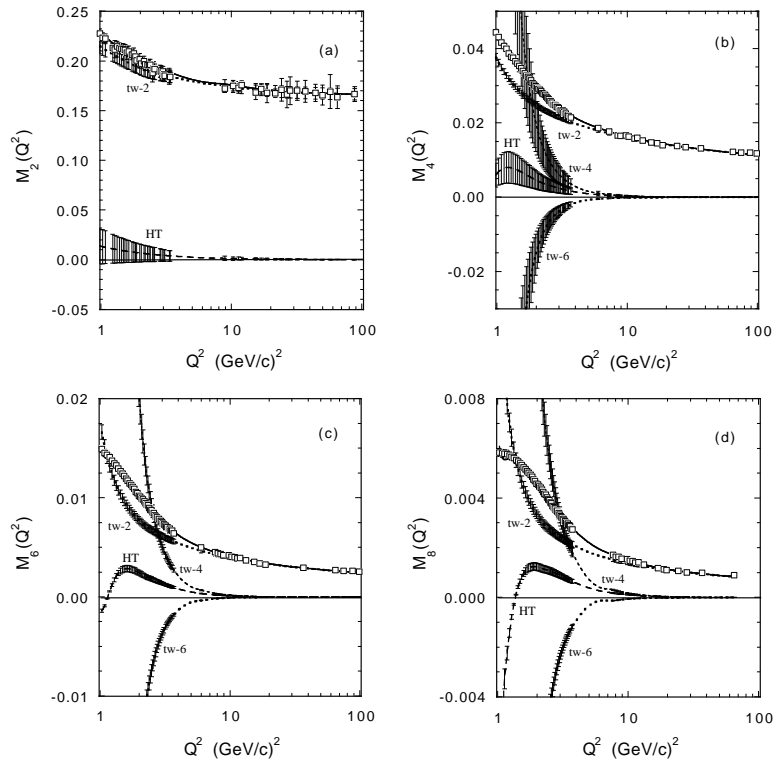
- Jlab provides unprecedented precision for structure function measurements.
- Data must be used in global analyses that include all the world's data.
- There is room for more precise data here.

## CLAS Unpolarized Moments



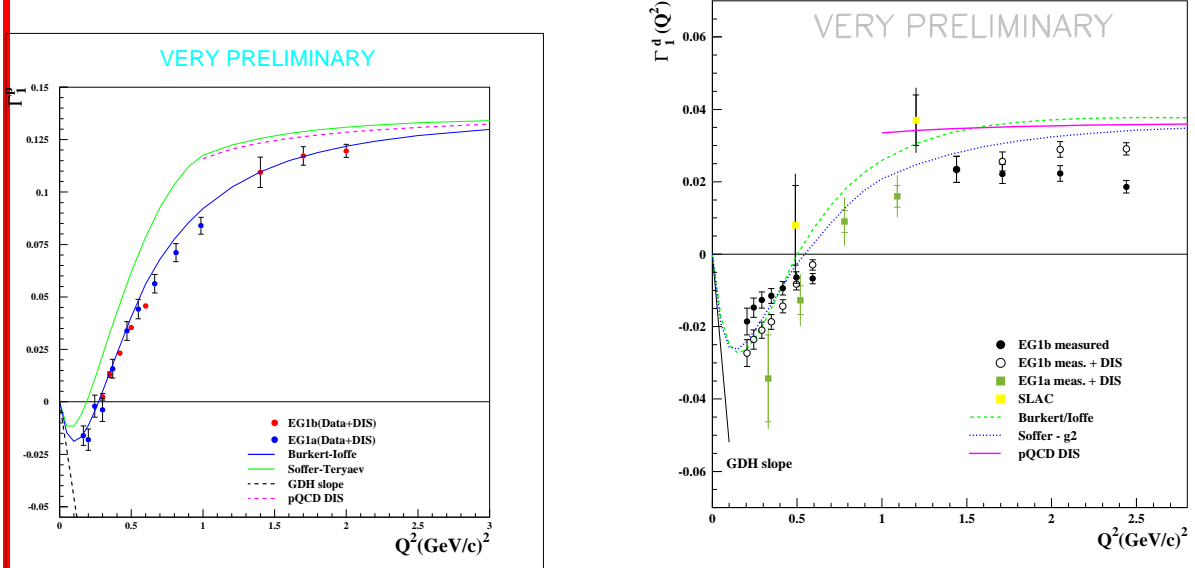
- Any function is known by its moments [e.g.  $M_n = \int_0^1 dx x^n f(x)$ ].
- Nachtmann moments:  $M_n(Q^2) = \int_0^1 dx C \frac{\xi^{n+1}}{x^3} F_2(x, Q^2)$  in which  $C = [3 + 3(n+1)r + n(n+2)r^2]/[(n+2)(n+3)]$ ,  $r = \sqrt{1 + 4M^2 x^2/Q^2}$ , and  $\xi = 2x/(1+r)$ .
- Operator Product Expansion:  $M_n(Q^2) = A_n(Q^2) + \sum_{k=1}^{\infty} \left(\frac{n\beta^2}{Q^2}\right)^k B_{nk}(Q^2)$ , in which  $\beta$  is the scale constant for higher twist effects.

## CLAS Unpolarized Moments

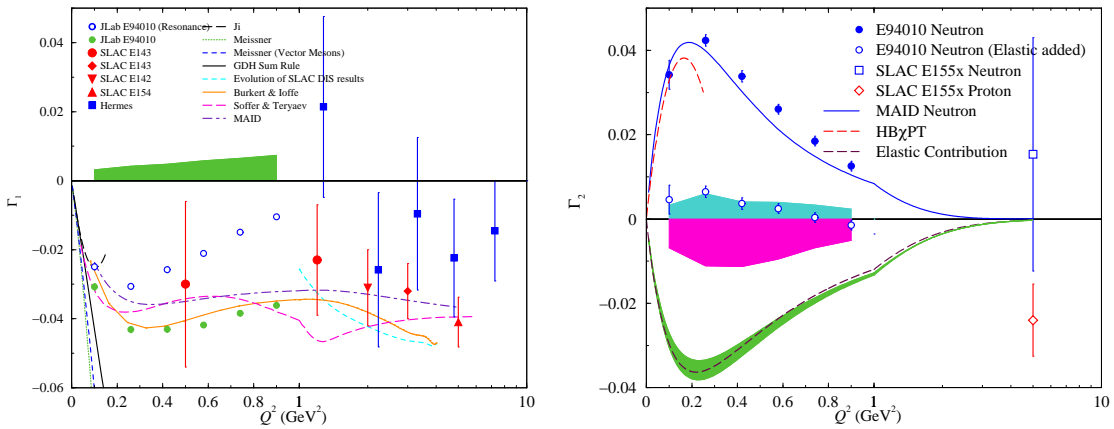


- Higher twist implies multi-parton correlations.
- Inelastic moments fit to powers of  $1/Q^2$ .
- Higher twist is important (especially for the higher moments) up to  $Q^2 = 8\text{-}10 \text{ GeV}^2$ .

## $\Gamma_1$ and $\Gamma_2$ vs. $Q^2$

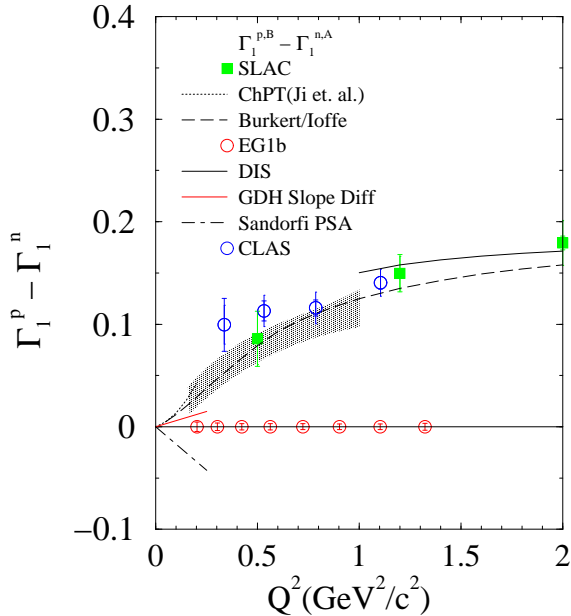


First polarized moment  $\Gamma_{1,2} = \int_0^1 g_{1,2}(x, Q^2) dx$



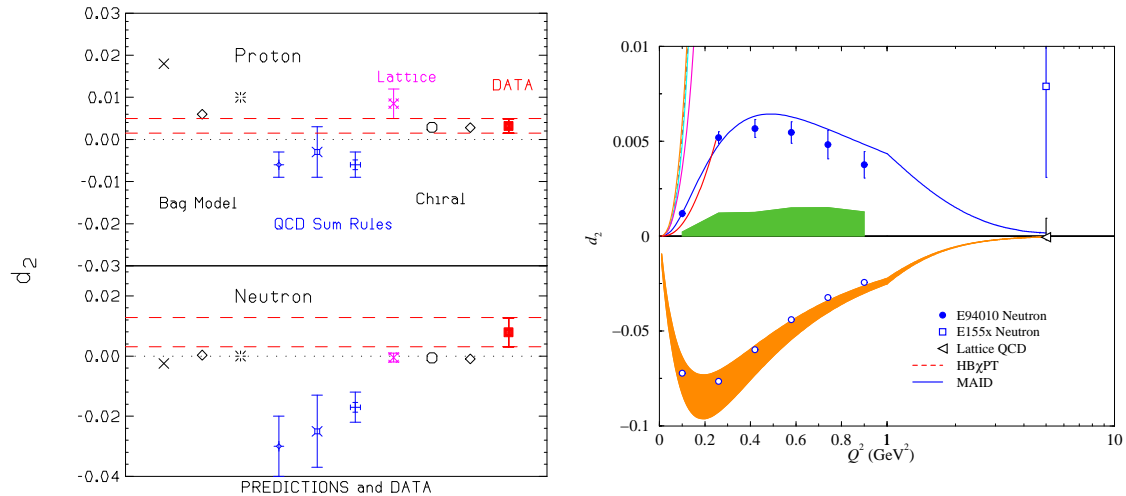
$$\Gamma_1^p - \Gamma_1^n$$

### The Bjorken Sum Rule



- Bjorken Sum Rule:  $\Gamma_1^p - \Gamma_1^n = \frac{1}{6}g_A C_{ns}$
- $C_{ns}$  evolves with  $Q^2$ .
- At low  $Q^2$  where resonances dominate, the pQCD extrapolation fails.
- Data are presently being analyzed that will make a precise measure of the Bjorken sum below  $Q^2 \approx 1 \text{ GeV}^2$ .

## Higher Twist Coefficient $d_2$



OPE up to twist-3:

$$\Gamma_1^{(n)} = \int_0^1 x^n g_1(x, Q^2) dx = \frac{a_n}{2}$$

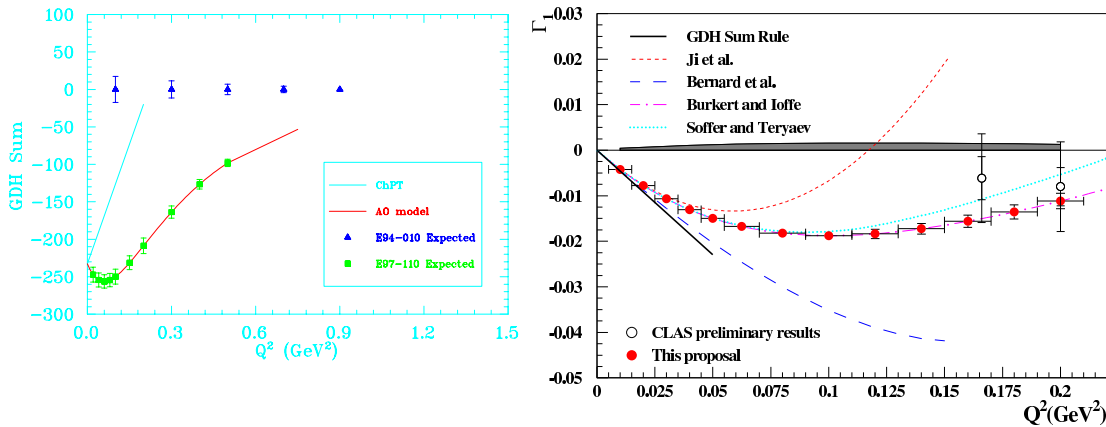
$$\Gamma_2^{(n)} = \int_0^1 x^n g_2(x, Q^2) dx = \frac{1}{2} \frac{n}{n+1} (d_n - a_n)$$

$$d_n = 2 \int_0^1 x^n \left[ g_1 + \frac{n+1}{n} g_2 \right] dx$$

Left curve: E155x at SLAC

Right curve: Hall A E94-010

## Future GDH Measurements



- Hall A will extend its polarized neutron structure function measurements to low  $Q^2$  by using a septum magnet to get down to  $6^\circ$  scattering angles (left graph).
- Hall B will extend its polarized proton structure function measurements to low  $Q^2$  by using a new small-angle Cherenkov counter (right graph).
- Together, these experiments will map out the approach to the Gerasimov-Drell-Hearn (GDH) limit.
- GDH extrapolation shows  $\Gamma_1 \rightarrow -\kappa^2 Q^2 / 8M^2$  as  $Q^2 \rightarrow 0$ .

## Conclusions

- Jlab results show exceptional precision and kinematic coverage for both unpolarized and polarized structure functions in the resonance region and beyond.
- Proper understanding in the framework of QCD requires an expansive data set for which the determination of moments of structure functions can be done without excessive extrapolation. This is now possible with JLab data.
- These high-quality data from JLab provide the framework for understanding the complex region between chiral and QCD perturbative descriptions.
- With the upgrade in energy and new techniques for measuring the neutron, JLab can effectively provide a complete set of data at low  $Q^2$  that ties directly to the world's DIS data.